energies

MDPI

Article

Entropy Analysis of EMHD Hybrid Nanofluid Stagnation Point Flow over a Porous Stretching Sheet with Melting Heat Transfer in the Presence of Thermal Radiation

J. Kayalvizhi and A. G. Vijaya Kumar *

Department of Mathematics, School of Advanced Sciences, Vellore Institute of Technology, Vellore 632014, India
* Correspondence: vijayakumarag@vit.ac.in

Abstract: In this study, the entropy formation of an electromagnetohydrodynamic hybrid nanofluid at a stagnation point flow towards a stretched surface in the presence of melting heat transfer, second-order slip, porous medium, viscous dissipation and thermal radiation are investigated. Hybrid nanoparticles alumina (Al_2O_3) and copper (Cu) are considered, with the base fluid water (H_2O). Similarity transformations are used to address the governing partial differential equations (PDEs) that lead to the corresponding ordinary differential equations. The resulting ODEs are solved by employing bvp4c solver numerically in the MATLAB package. The effects of temperature, transport, production of entropy and Bejan number *Be* are graphically exhibited. Higher radiation parameters *R* and an electric field *E* lead to an increase in fluid temperature. The velocity boundary layer is lowered by the magnetic field and porous media parameters. The opposite behaviour is observed in the electric field *E*. As a result, hybrid nanofluid has numerous uses in engineering cosmetics, automotive industry, home industry, for cancer treatment, food packaging, pharmaceuticals, fabrics, paper plastics, paints, ceramics, food colorants, electronics, heat exchangers, water purification, lubricants and soaps as well.

Keywords: hybrid nanofluid; electric field; magnetic field; radiative heat flux; porous medium; viscous dissipation; entropy generation

Citation: Kayalvizhi, J.; Vijaya Kumar, A.G. Entropy Analysis of EMHD Hybrid Nanofluid Stagnation Point Flow over a Porous Stretching Sheet with Melting Heat Transfer in the Presence of Thermal Radiation. *Energies* **2022**, *15*, 8317. https://doi.org/10.3390/en15218317

Received: 27 September 2022
Accepted: 1 November 2022
Published: 7 November 2022

1. Introduction

Nanotechnology is gaining popularity as a result of its important function of improving the heat capacity of liquids by boosting heat and mass transfer rates. Due to its wide variety of applications in heat exchangers, biomedicine, electronic device cooling, food, double windowpane, transportation, and other fields, the idea of nanofluids has become a more expansive topic for the research community in recent years. To improve the heat capacity of common fluids like kerosene, water, and motor oil, etc., nanoparticles of different kinds must be included in the base fluids, such as graphene, silica, alumina, gold, copper, silver, carbon nanotubes, and so on. It is suggested by Choi [1] that the word nanofluid should be used to characterize the thermal conductivity of the suspension in the base fluid that is enhanced by the particle dispersion in the nanometer range. As discussed in a number of research publications that have been published in the literature, the addition of different kinds of nanoparticles may increase the thermal conductivity of base fluids. H_2O-Cu and H_2O-Ag nanofluids are used by Kaneswaran et al. [2] to investigate the influence of relevant factors on the MHD nanofluid flow across an extending sheet. The effects of viscosity dissipation and chemical reaction are taken into account, it is found that the rate of heat and mass transfers of H_2O-Cu are higher. Kumaresan and Kumar [3] explored chemically reactive 3d magneto hydrodynamic rotating flow of nanofluids across a deformable surface with joule heating through pores media. Hybrid nanofluids are a new type of nanofluid that has lately received a lot of attention. It is recognized that due to a combination of components, hybrid nanofluids have better thermal characteristics. In

continuation hybrid nanofluids is a mixed nanofluids, which blend or mix two distinct kinds of nanoparticles. Jana et al. [4] conducted an experimental analysis of this fluid type in 2007. In particularly, these hybrid nanofluids are play a significant part in a wide variety of applications, including solar water heating, heat exchangers, vehicle brake fluids, defense, medical, manufacturing, microfluidics and microelectronics, amongst others.

Several studies have been conducted in order to better understand the heat transmission characteristics of hybrid nanofluids. The combined effects of melting heat transfer and viscous dissipation on MHD hybrid nanofluid flow are discussed by Kumar [5]. Suresh et al. [6,7] studied the convective heat exchange of Cu-Al_2O_3/water hybrid nanofluids via a circular pipe. For the Al_2O_3-Cu/H_2O hybrid nanofluid, the average rise in Nusselt number was 8.02%, which is much higher than that of the basic fluid (H_2O). The friction factor of Al_2O_3-Cu/H_2O hybrid nanofluids is somewhat greater than that of Al_2O_3/H_2O nanofluids, according to the findings of the experiments. As part of his research, Bhattad [8] consider a experimnental investigation of aluminium oxide–magnesium oxide hybrid nanofluid in a plate heat transfer. He looked at the exergy–energy properties of the nanofluid. The optimal temperature range for a hybrid nanofluid is 30–45° Celsius with a flow rate of 2.0–4.0 L/min. Deionized H_2O (4:1) hybrid nanofluid of alumina and magnesium oxide increased the heat exchanger performance index by 11.1%, according to the study's findings. Some references [9–11] provided a few studies on nanofluids.

The study of the movement of electrically conducting fluid under the impact of magnetic and electric fields is known as electromagnetohydrodynamics. The Lorentz force is also active and interacts with the buoyancy force in regulating the flow and temperature fields when the fluid is electrically conducting and a magnetic field is applied. The Lorentz force reduces the velocities of convection currents; adding an external magnetic field may be used as a control tool in the material-building sector. Due to the many different fields that electromagnetohydrodynamic may be used in, including biomedical engineering, geophysics, magnetic drug targeting, engineering, and many more, there has been interest in the field in recent years. According to Shah et al. [12], heat radiation has a significant impact on the EMHD rotational flow of carbon nanotubes across a stretched sheet, and they discovered that the electric and magnetic parameters move in opposite directions along the momentum boundary layer. In their analysis of the 2D unstable electromagnetohydrodynamic nanofluid flow over an extending sheet with multislip and dual stratification effects, Daniel et al. [13] found that the parameter of the electric field has a positive impact on the velocity boundary. Electromagnetohydrodynamics was computationally investigated by Abbas et al. [14] in a flow of nanofluid across a porous Riga plate for gyrotactic microorganisms. Jakeer [15] examined the irreversibility analysis of an electromagnetohydrodynamic Al_2O_3-Cu/H_2O nanofluid at a stagnation point in the presence of thermal radiation and viscous dissipation. References [16,17] provide a few studies on electromagnetohydrodynamic.

Many researchers are interested in discovering EMHD in heat transport with radiation and viscous dissipation impac due to its vast variety of applications. It is used in astrophysics and geophysics to investigate stellar and solar structures as well as radio transmission via the ionosphere. It has uses in engineering, such as MHD pumps and MHD bearings engineering. Thermal radiation plays an immense role in surface heat transfer, it is used in manufacturing, the design of dependable equipment, nuclear power plants, gas turbines, aeroplanes, missiles, satellites, space vehicles, space technologies, and procedures involving high temperatures. In the medical field lukewarm radiation is in high demand. The impact of thermal radiation with double diffusion has been an important research issue for many experimenters because of its use in medical therapy. Infrared radiation is a common kind of heat treatment that is useful in many different parts of the human body it is produced by oscillations in the electromagnetic field. Radiative heat transfer allows electromagnetic waves to carry vitality. Visible brightness and microwaving are related; it helps with a variety of skin issues. The wavelength of radiation penetrating skin is determined by its radiating structure, vascularity and pigmentation. Heat treatment is

aided by infrared radiation, which warms the afflicted area's blood capillaries directly. It improves the body's blood flow, which helps to prevent infection in superficial wounds. It also draws attention to white blood cells while removing waste products. Studies on mass and heat transmission fluid flow in porous media have a variety of applications in the field of thermal technology. A few of these applications include geothermal energy recuperation, extraction of unrefined petroleum, thermal energy storage, ground water hydrology, thermal insulation, ceramic engineering flow through filtering devices, and so on.

Electromagnetohydrodynamic (EMHD) effects on corrugated walls in microchannels through the porous medium is studied by Rashid et al. [18]. Using an expanding/shrinking surface, Zheng et al. [19] investigated the boundary layer flow and radiative transport of an incompressible micropolar liquid. Warke et al. [20] examined the effects of porous media on the mass and heat transfer of mixed convective–radiative magneto micropolar liquid flow across a vertical surface. Daniel et al. [21] analysed slip and convective conditions on MHD nanofluid flow through a porous stretching and shrinking sheet. Tripathi et al. [22] explored the effect of Coriolis body force, electromagnetohydrodynamic (EMHD) and thermal radiative heat transfer on the Casson hybrid mixed convection nanofluid propelled by an exponentially accelerated plate next to a porous medium in a rotating system. Singh et al. [23] presented the solutions of a chemically reacting and melting heat transfer on non-Newtonian flow near the stagnation point in a porous medium with nonuniform heat sources and sinks. Khatun et al. [24] conducted a computational examination of the nature of electromagnetohydrodynamic (EMHD) radiating fluid flow over an infinitely long vertical Riga plate in a rotating environment.

In heat transport analysis, viscous dissipation is important, especially in boundary layer flow. As a result of higher velocity gradients (V-G) in boundary layer flow, the lower temperature functions as a heat source, resulting in a considerable rise in fluid temperature. The kinetic energy of the liquid is converted to heat energy when it passes through the boundary layer flow due to the larger gradations in velocity inside the liquid flow. Several manufacturing and technical applications necessitate the study of fluid flow in a porous medium, including irrigation and drainage, extraction of gas or fuel, petrochemicals, flow of blood, cosmetic products, extraction of particulates from soils and specific separation mechanisms such as filtering and absorption in industrial engineering. Using viscous dissipation, Mallikarjuna et al. [25] investigated the impact of melting heat transfer and viscous dissipation on the two-phase flow of a dusty hybrid nanofluid using the Forchheimer–Darcy model. The movements of blood conveying Au nanosized particles are valuable to the field of medication during the testing process. Aanalysis of Koriko et al. [26] states, the space experts found that the impact of conveying dust particles over rockets was helpful in air dynamics. First time, Gebhart et al. [27] noticed an increase in the temperature of fluid with a convective heat transmission rate. Awais et. al. [28] Investigate the impact of organisms on the exploration of heat, stratification and viscous dissipation in bio-convectional nanomaterials. Industrial operations of a higher level and viscosity dissipation on nanofluids with a continuous stretchy medium of porous are reported by Gopal et al. [29]. Aziz et al. [30] presented hybrid Powell–Eyring nanofluid entropy production.

To the best of authors knowledge, the idea of electromagnetohydrodynamics hybrid nanofluid flow across a stretching surface with melting heat transfer, thermal radiation, entropy generation and stagnation point not yet been addressed. For this hybrid nanofluid flow, both electric and magnetic field are considered. In addition, the effects of viscous dissipation and thermal radiation are studied in heat transfer in order to assess their relevance in the heat transfer process. The Runge–Kutta fourth order, along with the shooting technique, are applied to execute the results of modelled energy and momentum equations. Finally, with the use of tables and graphs, the physical characteristics of the necessary parameters are investigated. In addition, profiles of entropy generation have been drafted. This model might be good for cancer therapy because cancer cells make a

large amount of heat; so, the entropy of cancer cells is very high. This means that analyzing tumor cells can help in healing their surrounding healthy cells.

2. Mathematical Formulation

Consider a stable, incompressible, two-dimensional, electrically conductive hybrid nanofluid and stagnation point flow over a stretched sheet coated in a permeable medium in the presence of thermal radiation and viscous dissipation, as shown in Figure 1.

- The velocity of the stretching sheet is $u_w(x) = cx$ and the outer flow velocity of is $u_e(x) = \omega x$, where ω and c both are positive constants.
- The boundary layer equations of the fluid flow are composed from the continuity equation, the momentum equation and the energy equation, which are formulated based on Maxwell's equation and Ohm's law.
- The effects of a magnetic field B and an electric field E on the incompressible flow of a viscous fluid are considered.
- The magnetic and electric fields obey Ohm's law defining magnetic induction as $\vec{J} = \sigma\left(\vec{E} + \vec{v} \times \vec{B}\right)$, where σ is the electric conductivity, $\vec{v}$ represents the fluid velocity and $\vec{J}$ flui the current.
- The melting surface and ambient temperature are represented by T_m and T_∞, where $T_m < T_\infty$.
- A magnetic field and electric field are applied normal to the flow, such that the Reynolds number is assumed to be smaller. The induced magnetic field is smaller than applied magnetic field. As a result, for low magnetic Reynolds numbers, the induced magnetic field is ignored.
- Entropy analysis is also taken into account.
- As a result of the above analysis, the flow is governed by [31–33].

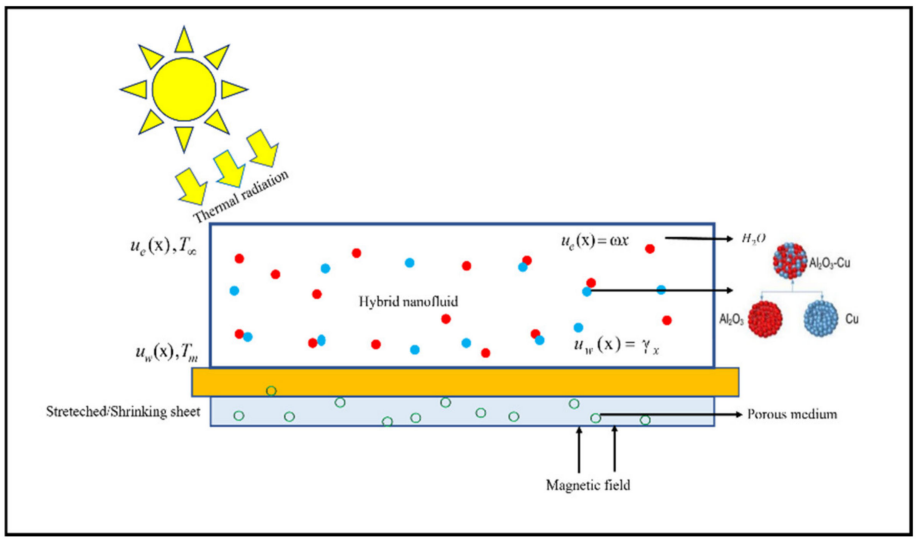

Figure 1. Configuration of the flow model.

$$\frac{\partial u}{\partial x} + \frac{\partial v}{\partial y} = 0 \tag{1}$$

$$u\frac{\partial u}{\partial x} + v\frac{\partial v}{\partial y} = u_e\frac{du_e}{dx} + \frac{\mu_{hnf}}{\rho_{hnf}}\frac{\partial^2 u}{\partial y^2} + \frac{\sigma_{hnf}}{\rho_{hnf}}\left(E_0B_0 - B_0^2(u_e - u)\right) - \frac{\mu_{hnf}}{\rho_{hnf}\,K^*}(u_e - u) \tag{2}$$

$$u\frac{\partial T}{\partial x}+v\frac{\partial T}{\partial y}=\frac{k_{hnf}}{(\rho c_p)_{hnf}}\frac{\partial^2 T}{\partial y^2}+\frac{\mu_{hnf}}{(\rho c_p)_{hnf}}\left(\frac{\partial u}{\partial y}\right)^2-\frac{1}{(\rho c_p)_{hnf}}\frac{\partial q_r}{\partial y}+\frac{\sigma_{hnf}}{(\rho c_p)_{hnf}}(uB_0-E_0)^2+\frac{Q_0}{(\rho c_p)_{hnf}}(T-T_\infty) \tag{3}$$

The adequate corresponding initial and boundary conditions are given by [31].

$$u=u_{slip}+u_w(x), T_m=T$$

$$T\to T_\infty\ u\to u_e(x)\ y\to\infty \tag{4}$$

$$k_{hnf}\left(\frac{\partial T}{\partial y}\right)_{y=0}=\rho_{hnf}[c_s\ (T_m-T_0)+L]v(x,0) \tag{5}$$

The thermophysical characteristics of [34] hybrid nanofluids are specified as follows:

$$\frac{k_{hnf}}{k_f}=\frac{2(1-\phi)k_{f+}(1+2\phi_{1s})k_{1s}+(1+2\phi_{2s})k_{2s}}{(2-\phi)k_{f+}(1-\phi_1)k_{1s}+(1-\phi_2)k_{2s}},\ \frac{\mu_{hnf}}{\mu_f}=(1-\phi)^{-2.5}$$

$$\frac{\rho_{hnf}}{\rho_f}=(1-\phi)+\frac{\phi_{1s}\rho_{1s}}{\rho_f}+\frac{\phi_{2s}\rho_{2s}}{\rho_f},\quad \frac{(\rho c_p)_{hnf}}{(\rho c_p)_f}=(1-\phi)+\frac{\phi_{1s}(\rho c_p)_{1s}+\phi_{2s}(\rho c_p)_{2s}}{(\rho c_p)_f} \tag{6}$$

$$\frac{\sigma_{hnf}}{\sigma_f}=\left[1+\frac{3\sigma_{1s}\phi_{1s}+\phi_{2s}\sigma_{2s}-3\phi\sigma_f}{\sigma_{1s}(1-\phi_{1s})+\sigma_{2s}(1-\phi_{2s})+(2+\phi)\sigma_f}\right],\quad \phi=\phi_{1s}+\phi_{2s}$$

Here, u and v are the velocity components of x and y axes T and L represent the hybrid nanofluid's temperature and latent heat. Roberts [35] established the melting surface condition in Equation (5) c_s denotes heat capacity. Furthermore, Lin Wu [36] develops and defines the velocity slip as follows.

$$u_{slip}=A\frac{\partial u}{\partial y}+B\frac{\partial^2 u}{\partial y^2} \tag{7}$$

Famous astrophysicist Svein Roseland provided an approximation of radiation heat flux for a boundary layer that is optically thick as the following:

$$q_r^*=-\frac{4\sigma^*}{3k^*}\frac{\partial T^4}{\partial z} \tag{8}$$

where the Stefan–Boltzmann constant and Rosseland mean absorption coefficient are represented by σ^* and k^*, respectively, expanding Taylor's series on T^4 about the ambient temperature T_∞ as follows:

$$T^4={T_\infty}^4+4{T_\infty}^3(T-T_\infty)+6{T_\infty}^2(T-T_\infty)^2+\ldots \tag{9}$$

Since the temperature differences are very small in the natural convection process, the terms from second order onwards may be neglected, and then it takes the form of:

$$T^4\cong(4T-3T_\infty){T_\infty}^3 \tag{10}$$

From Equations (8)–(10), Equation (3) reduces to:

$$u\frac{\partial T}{\partial x}+v\frac{\partial T}{\partial y}=\frac{k_{hnf}}{(\rho c_p)_{hnf}}\frac{\partial^2 T}{\partial y^2}+\frac{\mu_{hnf}}{(\rho c_p)_{hnf}}\left(\frac{\partial u}{\partial y}\right)^2+\frac{16\sigma^*{T_\infty}^3}{(\rho c_p)_{hnf}3K^*}\frac{\partial^2 T}{\partial y^2}+\frac{\sigma_{hnf}}{(\rho c_p)_{hnf}}(uB_0-E_0)^2+\frac{Q_0}{(\rho c_p)_{hnf}}(T-T_\infty) \tag{11}$$

To obtain ordinary differential equations, we exploited the following similarity transformations:

$$u = \omega x f'(\eta),\ v = -f(\eta)\sqrt{\left(\omega v_f\right)}, \frac{T - T_m}{T_\infty - T_m} = \theta(\eta),\ \eta = y\left(\frac{\omega}{v_f}\right)^{1/2} \tag{12}$$

By using similarity variables (12), Equations (2) and (11) transformed as:

$$\frac{A_1}{A_2}f''' + ff'' - f'^2 + 1 + \frac{A_3}{A_2}M\left(E - \left(1 - f'\right)\right) + \frac{A_1}{A_2}K(1 - f') = 0 \tag{13}$$

$$\frac{A_4}{Pr}\left(A_5 + \frac{4}{3}R\right)\theta'' + \frac{A_1}{A_4}Ecf''^2 + f\theta' + \frac{A_3}{A_4}MEc(f' - E)^2 + \frac{1}{A_4}Q\theta = 0 \tag{14}$$

The nondimensional boundary conditions are taken into consideration:

$$\left.\begin{array}{l} f(0)Pr\frac{\rho_{hnf}}{\rho_f} + \theta'(0)M_1\frac{k_{hnf}}{k_f} = 0, \\ f(0) = f'''(0)\beta + f''(0)\alpha + \lambda, \quad \theta(0) = 0 \quad as \quad \eta \to 0 \\ f'(\eta) \to 1, \theta(\eta) \to 1, \quad as \quad \eta \to \infty \end{array}\right\} \tag{15}$$

Together with the corresponding nondimensional parameters, are given

$$\begin{array}{c} Pr = \frac{(\mu C_P)_f}{k_f},\ \alpha = A\sqrt{\frac{\omega}{v_f}},\ \beta = \frac{\omega B}{v_f},\ M_1 = \frac{(T_\infty - T_m)(C_P)_f}{L + (T_m - T_0)c_s},\ E = \frac{E_0}{\beta_0 u_e}, \\ M = \frac{\sigma_f \beta_0^2}{\rho_f \omega},\ Ec = \frac{\omega x^2}{C_p \Delta T},\ K = \frac{\gamma_f}{wk^*},\ R = \frac{4\sigma^* {T_\infty}^*}{K^* k_f},\lambda = \frac{\gamma}{\omega},\ Q = \frac{Q_0}{w}. \end{array} \tag{16}$$

The mathematical kinds of constants A_1, A_2, A_3, A_4 and A_5 may now be expressed as follows:

$$\left.\begin{array}{l} A_1 = \mu_{hnf}/\mu_f,\ \ A_2 = \rho_{hnf}/\rho_f,\ A_3 = \sigma_{hnf}/\sigma_f \\ A_4 = (\rho c_p)_{hnf}/(\rho c_p)_f,\ \ A_5 = k_{hnf}/k_f \end{array}\right\} \tag{17}$$

The C_f is the friction drag coefficient and Nu_x is the local rate of heat transmission, as follows:

$$C_f = \frac{\mu_{hnf}}{\rho_f u_w^2}\left(\frac{\partial u}{\partial y}\right)\Big|_{y=0}, \quad Nu_x = -\frac{k_{hnf}xq_w}{k_f\left(T_f - T_\infty\right)}\left(\frac{\partial T}{\partial y}\right)\Big|_{y=0} \tag{18}$$

Using Equations (7) and (14), we obtained

$$c_f(\mathrm{Re}_x)^{1/2} = \frac{1}{(1 - \phi_1)^{2.5}(1 - \phi_2)^{2.5}}f''(0) \tag{19}$$

$$Nu_x(\mathrm{Re}_x)^{1/2} = -\left(\frac{k_{hnf}}{k_f} + \frac{4}{3}R\right)\theta'(0) \tag{20}$$

Here, $\mathrm{Re}_x = \frac{u_e x}{\gamma_f}$ is the local Reynolds number.

3. Entropy Analysis or Analysis of Energy Loss

Entropy generation in a hybrid nanofluid with the effects of electric field, magnetic field and thermal radiative heat flow is characterized as follows [37–39]:

$$S_G = \underbrace{\frac{1}{{T_\infty}^2}\left(K_{hnf} + \frac{16\sigma^* {T_\infty}^3}{3k^*}\right)\left(\frac{\partial T}{\partial y}\right)^2}_{\substack{energy\ loss\ via \\ heat\ transfer}} + \underbrace{\frac{\mu_{hnf}}{T_\infty}\left(\frac{\partial u}{\partial y}\right)^2}_{\substack{energy\ loss\ via \\ fluid\ friction}} + \underbrace{\frac{\sigma}{T_\infty}(uB_0 - E_0)^2}_{\substack{energy\ loss\ via \\ Joule\ dissipation\ and \\ electric\ field}} \tag{21}$$

Using Equation (7), Equation (16) yields the regenerated dimensionless form as follows:

$$N_G = \left(\frac{K_{hnf}}{K_f} + \frac{4}{3}R\right)\alpha_1\theta'^2 + Br\,(1-\phi_1)^{-2.5}(1-\phi_2)^{-2.5}f'' + M\,Br\,\left(f'-E\right)^2 \quad (22)$$

where, the local entropy is $N_G = \frac{S_G\ \gamma_f\ T_\infty}{K_f\ \omega\ \Delta T}$, $\alpha_1 = \frac{\Delta T}{T_\infty}$ is the dimensionless ratio variable, $Br = \frac{\mu_f\ {u_\omega}^2}{K_f\ \Delta T}$ is the Brinkman number.

The Bejan number is demonstrated as,

$$Be = \frac{\left(\frac{K_{hnf}}{K_f} + \frac{4}{3}R\right)\alpha_1\ \theta'^2}{\left(\frac{K_{hnf}}{K_f} + \frac{4}{3}R\right)\alpha_1\ \theta'^2 + \frac{Br}{(1-\phi_1)^{2.5}(1-\phi_2)^{2.5}}f'' + M\,Br(f'-E)^2} \quad (23)$$

4. Solution for Numerical Technique

The nondimensional system of Equations (13) and (14) as well as the boundary conditions (15) are numerically solved by using the Runge–Kutta fourth order along with shooting technique. Using similarity variables, the governing PDEs are converted into a set of ordinary differential equations and then transformed into a collection of first-order ODEs for this scheme. The detailed procedure is as follows

$$\begin{aligned}
&f = S_1\\
&f' = S_2\\
&f'' = S_3\\
&f''' = -\tfrac{A_2}{A_1}\left(S_1S_3 - (S_2)^2 + 1 + \tfrac{A_3}{A_2}M(E-(1-S_2)) + \tfrac{A_1}{A_2}K(1-S_2)\right)\\
&\theta = S_4\\
&\theta' = S_5\\
&\theta'' = -\tfrac{pr}{\left(A_5+\frac{4}{3}Rd\right)A_4}\ \left(\tfrac{A_1}{A_4}Ec(S_3)^2 + S_1S_5 + \tfrac{A_3}{A_4}M\,Ec(S_2-E)^2 + \tfrac{1}{A_4}QS_4\right)
\end{aligned}$$

Along with the boundary conditions are:

$$pr\ A_2\ S_1(0) + M_1\ A_5\ S_5(0) = 0$$

$$S_1(0) = \lambda + \alpha\psi(0) + \beta S_2(0),\ S_4(0) = 0,\ as\,\eta \to 0$$

$$S_2(\eta) \to 1,\ S_4(\eta) \to 1\ \text{ as } \eta \to \infty$$

Where,

$$\psi = f''' = -\tfrac{A_2}{A_1}\left(S_1S_3 - (S_2)^2 + 1 + \tfrac{A_3}{A_2}M(E-(1-S_2)) + \tfrac{A_1}{A_2}K(1-S_2)\right)$$

Equations (13) to (14) are converted into first-order differential equations with the help of above expressions and also the boundary conditions we get

$$\begin{bmatrix} {s_1}' \\ {s_2}' \\ {s_3}' \\ {s_4}' \\ {s_5}' \end{bmatrix} = \begin{bmatrix} s_2 \\ s_3 \\ -\tfrac{A_2}{A_1}\left(S_1S_3 - (S_2)^2 + 1 + \tfrac{A_3}{A_2}M(E-(1-S_2)) + \tfrac{A_1}{A_2}K(1-S_2)\right) \\ s_5 \\ \theta'' = -\tfrac{pr}{\left(A_5+\frac{4}{3}Rd\right)A_4}\ \left(\tfrac{A_1}{A_4}Ec(S_3)^2 + S_1S_5 + \tfrac{A_3}{A_4}M\,Ec(S_2-E)^2 + \tfrac{1}{A_4}QS_4\right) \end{bmatrix}$$

5. Results and Discussion

This analysis has been accomplished to understand the physical mechanism of the present problems. On the governing model, computed numerical solutions and the computed values are plotted in terms of graphs and tables below. By using the Runge–Kutta 4th

order along with the shooting technique approach, a set of ordinary differential Equations (13) and (14) with regard to boundary conditions (15), are solved numerically. Not only that, the Bejan number is used to investigate entropy creation. The impacts of non dimensional factors, such as magnetic field M, porous medium K, electric field E, radiation parameter R, heat source/sink Q, Eckert number Ec, Bejan number Be and Brinkman number Br, on flow transport $f'(\eta)$ and fluid temperature $\theta(\eta)$ are discussed using graphs. Hybrid nanoparticles and base fluid physical parameters are listed in Table 1. Table 2 shows a good agreement between the numerical results bvp4c (MATLAB 2021b) compared with the HPM.

Table 1. Thermophoresis properties of water and nanoparticles [40].

Thermophysical Property	$\rho(kg/m^3)$	$C_p(J/kgK)$	$k(w/mK)$	$\sigma(\Omega m)^{-1}$
H_2O	997.1	4180	0.613	0.05
Cu	8933	385	401	59.5×10^6
Al_2O_3	3970	765	40	35×10^6

Table 2. Comparison of results of K with MATLAB and HPM for $\frac{1}{(1-\phi_1)^{2.5}(1-\phi_2)^{2.5}} f''$.

S. No	K	$\frac{1}{(1-\phi_1)^{2.5}(1-\phi_2)^{2.5}} f''$	
		MATLAB	HPM
1	0.0	1.000003	1.000003
2	0.1	1.000536	1.000195
3	0.2	1.000459	1.000402
4	0.3	1.000098	1.000086
5	0.4	1.000005	1.000019

The impact of the magnetic field parameter is seen in Figure 2. It is shown that hybrid nanofluid velocity has a negative impact on the function of M. According to an actual perspective, when the magnetic field M grows, it slows down the fluid by producing resistance in the flow direction known as the Lorentz force. Because the Lorentz force is shown in the radial direction, the flow velocity decreases due to the additional resistance, resulting in a decrease in the radial velocity field velocity. Figure 3 displays the velocity profiles for various values of porous medium K other parameters are constant. The thickness of the momentum boundary layer grows as K values increase, as indicated by the graph. The physical reason for this is that increasing K makes a porous medium less resistant, which improves the regime's momentum development and makes the fluid move faster.

As shown in Figure 4, the electric field E generated by the Lorentz force greatly improves the velocity profile of hybrid nanofluids. Figure 5 illustrates the influence of various values of M on dimensionless temperature. It is found that the temperature gradient increases as M increases. Physically, this results from the retarding characteristic of the external magnetic field that produces an opposing Lorentz force that prevents momentum transmission and increases the viscosity of the thermal boundary layer. According to Figure 6, raising the radiation parameter R causes an increase in fluid temperature and thermal radiation improves the fluid temperature throughout the boundary area. Because the thermal radiation parameter increases the amount of diffuse energy, the system remains stable.

Figure 7 depicts the effect of heat source/sink on the hybrid nanofluid's temperature. Specifically, the temperature rises as the heat source parameter increases. Figure 8 demonstrates that Ec values are increased, temperature profiles rise in the same way. Scientifically speaking, the Eckert number Ec is the ratio of the kinetic energy to the difference in specific enthalpy between the sheet and the fluid. Therefore, when the Eckert number increases,

work is done against the stresses of the viscous fluid to turn kinetic energy into internal energy. Because of this, increasing *Ec* makes the fluid temperature increase.

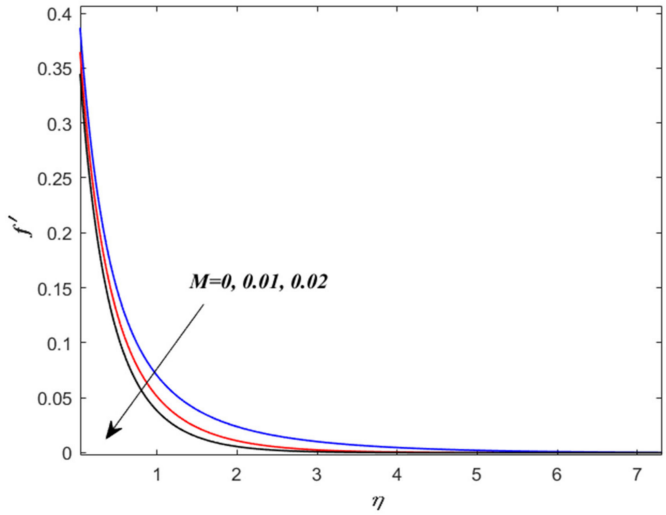

Figure 2. Various values of magnetic parameter (M) on velocity $f'(\eta)$.

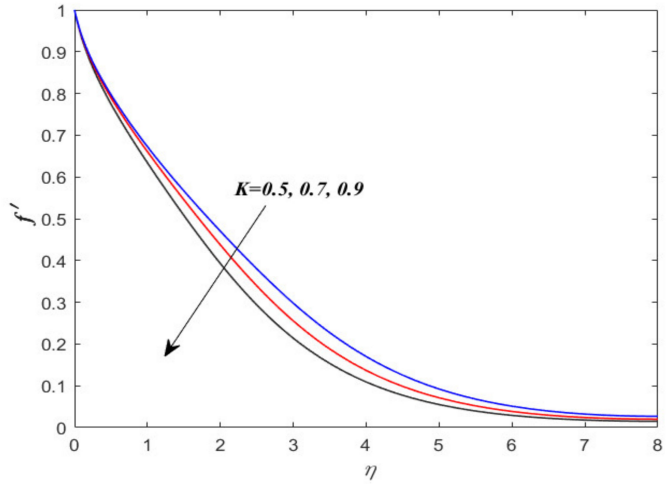

Figure 3. Various values of porous parameter (K) on velocity $f'(\eta)$.

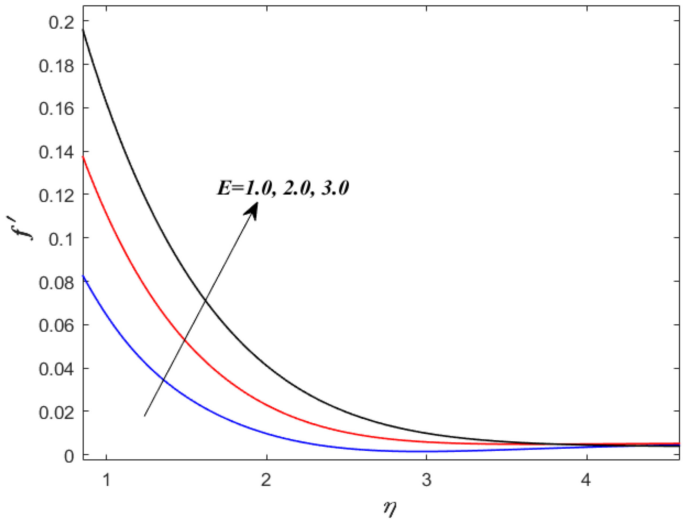

Figure 4. Various values of electric parameter (E) on velocity $f'(\eta)$.

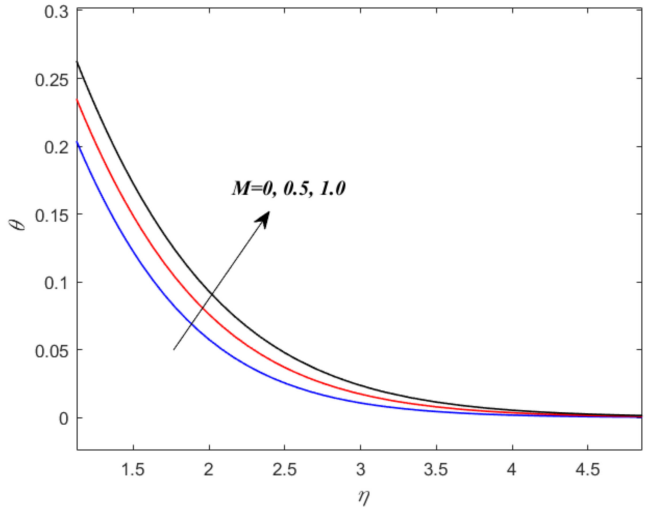

Figure 5. Various values of magnetic parameter (M) on temperature $\theta(\eta)$.

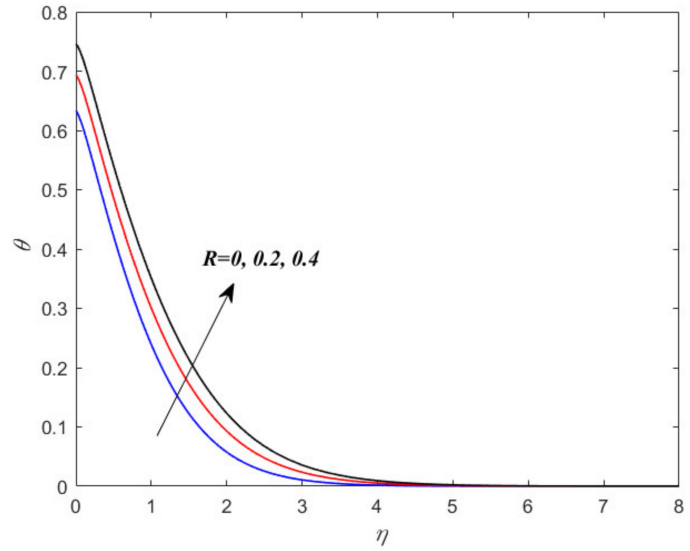

Figure 6. Various values of radiation parameter (R) on temperature $\theta(\eta)$.

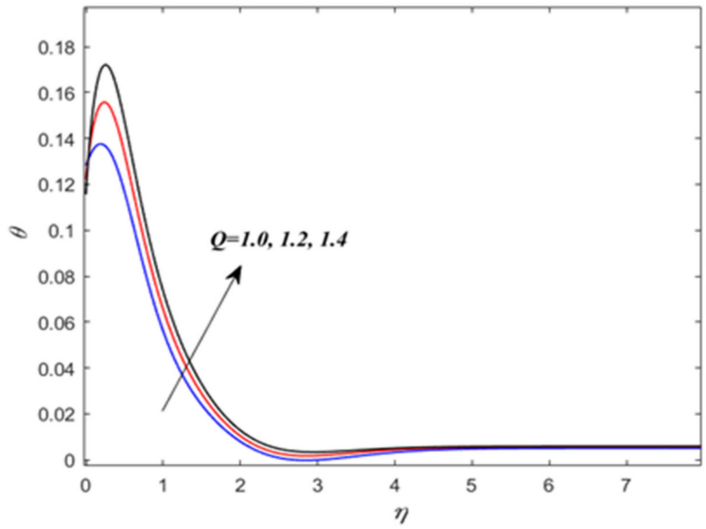

Figure 7. Various values of heat source parameter (Q) on temperature $\theta(\eta)$.

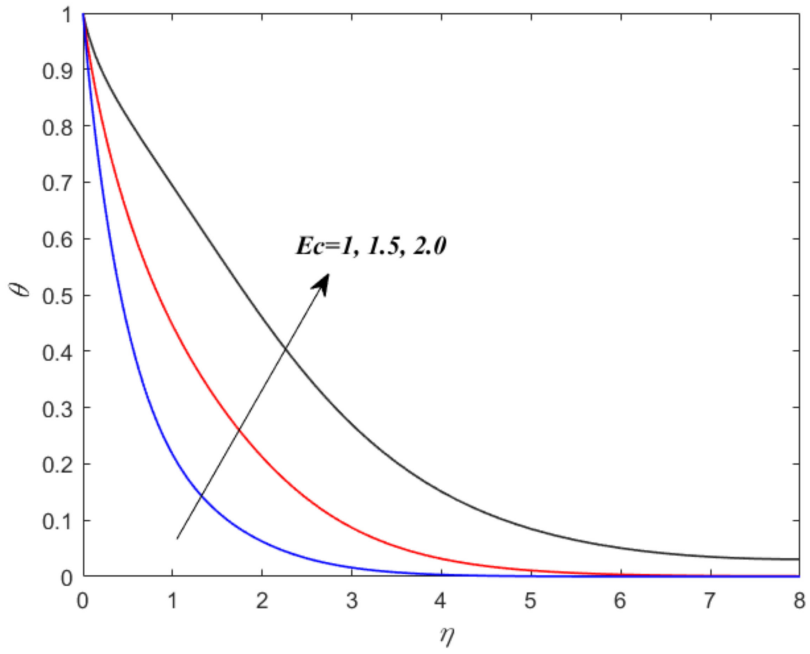

Figure 8. Various values of Eckert number (Ec) on temperature $\theta(\eta)$.

Figures 9–12 demonstrate the entropy profiles for the Brinkmann, radiation and magnetic parameters. The effect of the magnetic field M on the results of the entropy generation N_G is shown in Figure 9. Physically, there is greater friction when the magnetic parameter M causes the Lorentz force to grow. As a result, the rate of entropy generation (N_G) increases. Entropy generation rates are exemplified in Figure 10 for radiation parameter R. When R is increased to higher magnitudes, the thermal irreversibility also rises, which causes the system to become more disordered and causes N_G to rise. Figure 11 shows that the Bejan number decreases when the magnetic parameter is increased. Because of an increase in physical entropy production, the Bejan number drops. In Figure 12 displays the Bejan number is increased by varying the Brinkman number Br.

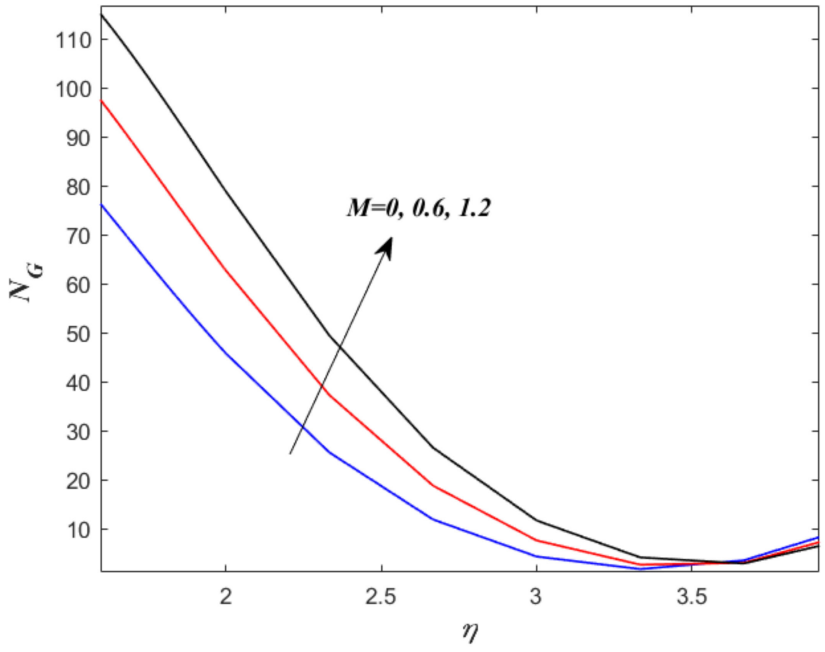

Figure 9. Various values of magnetic parameter (M) on N_G.

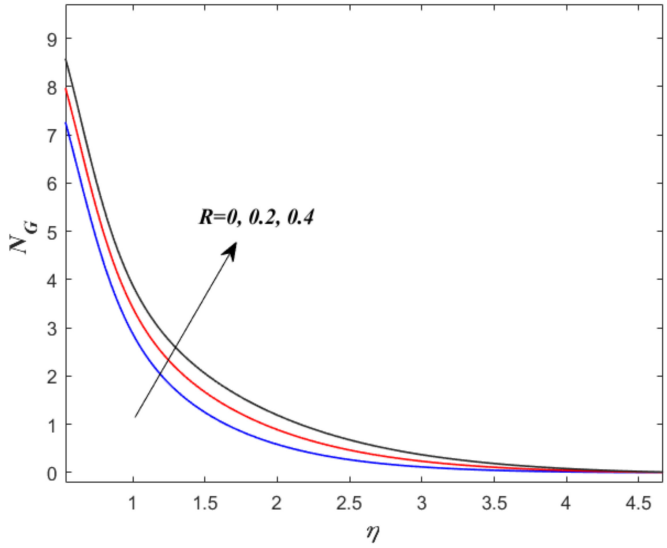

Figure 10. Various values of radiation parameter (R) on N_G.

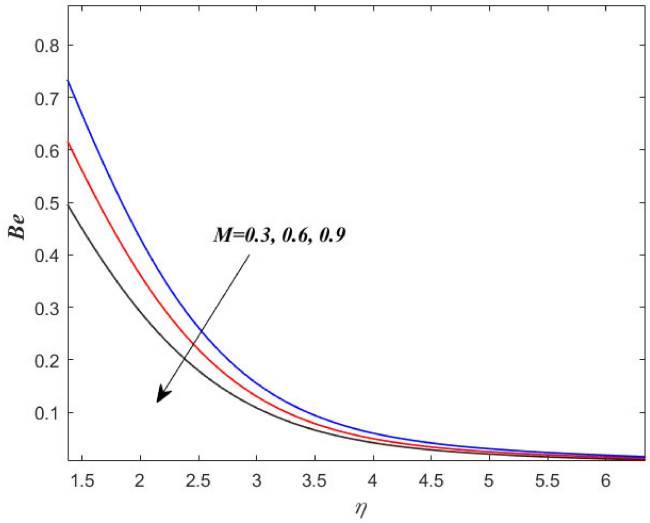

Figure 11. Various values of magnetic parameter (M) on Be.

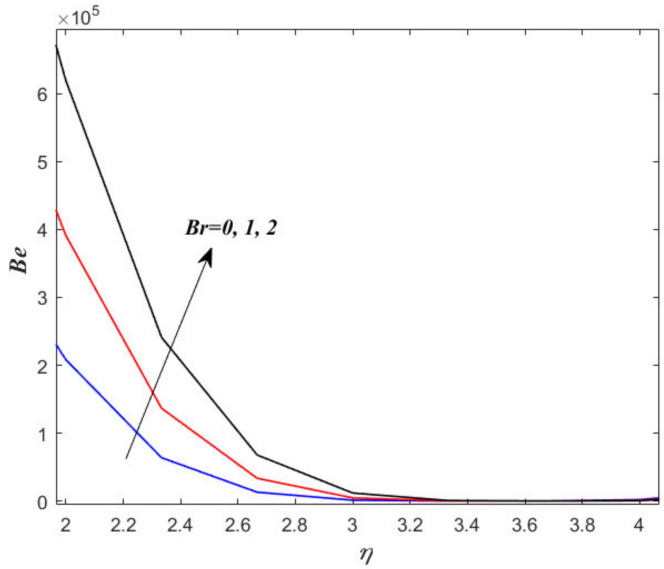

Figure 12. Various values of Brinkman number (Br) on Be.

6. Conclusions

The rate of entropy generation on EMHD $Cu - Al_2O_3/H_2O$ hybrid nanofluid at a stagnation point flow across a stretching surface is investigated in this paper. Second-order slip, porous medium, radiative heat flux, viscous dissipation and melting heat transmission are considered. A similarity solution method is employed to convert the dimensionless partial differential equations into a set of first - order ordinary differential equations. The resultant equations are solved numerically with the use of popular R-K method with shooting technique. The impacts of active factors on fluid transport, fluid temperature distribution, Bejan number and entropy generation are shown graphically.

The results of this latest investigation are summarized below.

- The velocity profile decreases when the magnetic parameter and porous medium are increased.
- As increasing the value of electric field, the momentum boundary layer is increases
- The thermal boundary layer expands as the magnetic parameter, radiation parameter, heat source and Eckert number are raised.
- Increases in radiation parameter and magnetic field cause an increase in the rate of entropy generation.
- The Bejan number rises as the Brinkman number rises, but the magnetic field shows the opposite trend.

Author Contributions: Conceptualization, J.K.; Data curation, J.K. and A.G.V.K.; Formal analysis, J.K.; Funding acquisition, A.G.V.K.; Investigation, J.K.; Methodology, J.K.; Project administration, A.G.V.K.; Software, J.K.; Supervision, A.G.V.K.; Validation, A.G.V.K.; Writing—original draft, J.K.; Writing—review & editing, A.G.V.K. All authors have read and agreed to the published version of the manuscript.

Funding: The authors are gratefully acknowledge the Vellore Institute of Technology management for providing a necessary facilities and support to carryout this research work.

Data Availability Statement: Not applicable.

Conflicts of Interest: The authors declare no conflict of interest.

Nomenclature

$A1, A2, A3, A4, A5$	Hybrid nanofluid constants
B_0	Magnetic field strength
B_e	Bejan number
Br	Brinkman number
c_f	Skin friction
E_0	Electric field strength (N/C)
E	Electric parameter
Ec	Eckert number
T	Temperature
T_w	Wall temperature
u_w	Velocity of the sheet
M	Magnetic parameter
M_1	Melting parameter
N_G	Local entropy generation
Nu_x	Local Nusselt number
R	Radiation parameter
pr	Prandtl number
K	Porous medium
Q	Parameter of heat source/sink
λ	Stretching parameter

Greek symbols	
β	Thermal expansion
μ	Viscosity
ρ	Density
σ	Electrical conductivity
ϕ	Volume fraction of nanoparticles
$(\rho c_p)_{hnf}$	Heat capacity of the hybrid nanofluid
$(\rho c_p)_f$	Heat capacity of the fluid
$(\rho c_p)_s$	Heat capacity of the nanoparticles' material
k_{hnf}	Thermal conductivity of the hybrid nanofluid
μ_{hnf}	Viscosity of hybrid nanofluid
γ_f	Fluid kinematic viscosity
Subscripts	
f	Fluid
hnf	Hybrid nanofluid
s	Solid particle
w	Condition at the sheet
∞	Ambient conditions.

References

1. Choi, S.U.S.; Eastman, J. Enhancing thermal conductivity of fluids with nanoparticles. In Proceedings of the 1995 ASME International Mechanical Engineering Congress & Exposition, San Francisco, CA, USA, 12–17 November 1995; pp. 99–105.
2. Kameswaran, P.K.; Narayana, M.; Sibanda, P.; Murthy, P.V. Hydromagnetic nanofluid flow due to a stretching or shrinking sheet with viscous dissipation and chemical reaction effects. *Int. J. Heat Mass Transf.* **2012**, *55*, 7587–7595. [CrossRef]
3. Kumaresan, E.; Vijaya Kumar, A.G. Chemically reactive 3D nonlinear magneto hydrodynamic rotating flow of nanofluids over a deformable surface with joule heating through porous medium. In *Applied Mathematics and Scientific Computing*; Springer: Cham, Switzerland, 2019; pp. 313–323.
4. Jana, S.; Salehi-Khojin, A.; Zhong, W.H. Enhancement of fluid thermal conductivity by the addition of single and hybrid nano-additives Lithium-Sulfur Batteries View project Lithium sulfur battery View project Enhancement of fluid thermal conductivity by the addition of single and hybrid nano-additives. *Thermochim. Acta* **2007**, *462*, 45–55.
5. Kumar, T.S. Hybrid nanofluid slip flow and heat transfer over a stretching surface. *Partial. Differ. Equ. Appl. Math.* **2021**, *4*, 100070. [CrossRef]
6. Suresh, S.; Venkitaraj, K.P.; Selvakumar, P.; Chandrasekar, M. Effect of Al_2O_3–Cu/water hybrid nanofluid in heat transfer. *Exp. Therm. Fluid Sci.* **2012**, *38*, 54–60. [CrossRef]
7. Suresh, S.; Venkitaraj, K.P.; Hameed, M.S.; Sarangan, J. Turbulent Heat Transfer and Pressure Drop Characteristics of Dilute Water Based Al_2O_3–Cu Hybrid Nanofluids. *J. Nanosci. Nanotechnol.* **2014**, *14*, 2563–2572. [CrossRef] [PubMed]
8. Bhattad, A. Experimental investigation of Al_2O_3–MgO hot hybrid nanofluid in a plate heat exchanger. *Heat Transf.* **2020**, *49*, 2344–2354. [CrossRef]
9. Selimefendigil, F.; Öztop, H.F.; Chamkha, A.J. MHD mixed convection and entropy generation of nanofluid filled lid driven cavity under the influence of inclined magnetic fields imposed to its upper and lower diagonal triangular domains. *J. Magn. Magn. Mater.* **2016**, ahead of print. [CrossRef]
10. Selimefendigil, F.; Öztop, H.F. Corrugated conductive partition effects on MHD free convection of CNT-water nanofluid in a cavity. *Int. J. Heat Mass Transf.* **2019**, *129*, 265–277. [CrossRef]
11. Sheremet, M.; Pop, I.; Öztop, H.F.; Abu-Hamdeh, N. Natural convection of nanofluid inside a wavy cavity with a non-uniform heating: Entropy generation analysis. *Int. J. Numer. Methods Heat Fluid Flow* **2017**, *27*, 958–980. [CrossRef]
12. Shah, Z.; Bonyah, E.; Islam, S.; Gul, T. Impact of thermal radiation on electrical MHD rotating flow of Carbon nanotubes over a stretching sheet. *AIP Adv.* **2019**, *9*, 15115. [CrossRef]
13. Daniel, Y.S.; Aziz, Z.A.; Ismail, Z.; Bahar, A. Unsteady EMHD dual stratified flow of nanofluid with slips impacts. *Alex. Eng. J.* **2020**, *59*, 177–189. [CrossRef]
14. Abbas, T.; Hayat, T.; Ayub, M.; Bhatti, M.M.; Alsaedi, A. Electromagnetohydrodynamic nanofluid flow past a porous Riga plate containing gyrotactic microorganism. *Neural Comput. Appl.* **2019**, *31*, 1905–1913. [CrossRef]
15. Jakeer, S.; Bala Anki Reddy, P. Entropy generation on EMHD stagnation point flow of hybrid nanofluid over a stretching sheet: Homotopy perturbation solution. *Phys. Scr.* **2020**, *95*, 125203. [CrossRef]
16. Ayub, M.; Abbas, T.; Bhatti, M.M. Inspiration of slip effects on electromagnetohydrodynamics (EMHD) nanofluid flow through a horizontal Riga plate. *Eur. Phys. J. Plus* **2016**, *131*, 193. [CrossRef]
17. Nayak, M.K.; Mabood, F.; Dogonchi, A.S.; Khan, W.A. Electromagnetic flow of SWCNT/MWCNT suspensions with optimized entropy generation and cubic auto catalysis chemical reaction. *Int. Commun. Heat Mass Transf.* **2021**, *120*, 104996. [CrossRef]

18. Rashid, M.; Shahzadi, I.; Nadeem, S. Corrugated walls analysis in microchannels through porous medium under Electromagneto-hydrodynamic (EMHD) effects. *Results Phys.* **2018**, *9*, 171–182. [CrossRef]
19. Zheng, L.; Niu, J.; Zhang, X.; Ma, L. Dual solutions for flow and radiative heat transfer of a micropolar fluid over stretching/shrinking sheet. *Int. J. Heat Mass Transf.* **2012**, *55*, 7577–7586. [CrossRef]
20. Warke, A.S.; Ramesh, K.; Mebarek-Oudina, F.; Abidi, A. Numerical investigation of the stagnation point flow of radiative magnetomicropolar liquid past a heated porous stretching sheet. *J. Therm. Anal. Calorim.* **2022**, *147*, 6901–6912. [CrossRef]
21. Daniel, Y.S.; Aziz, Z.A.; Ismail, Z.; Salah, F. Effects of slip and convective conditions on MHD flow of nanofluid over a porous nonlinear stretching/shrinking sheet. *Aust. J. Mech. Eng.* **2017**, *16*, 213–229. [CrossRef]
22. Prakash, J.; Tripathi, D.; Beg, O.A.; Srivastava, V. EMHD Casson Hybrid Nanofluid Flow over an Exponentially Accelerated Rotating Porous Surface. *J. Porous Media* **2022**, *25*, 1–24. [CrossRef]
23. Singh, K.; Kumar, M.; Pandey, A.K. Melting and chemical reaction effects in stagnation point flow of micropolar fluid over a stretchable porous medium in the presence of nonuniform heat source/sink. *J. Porous Media* **2020**, *23*, 767–781. [CrossRef]
24. Khatun, S.; Islam, M.M.; Mollah, M.; Poddar, S.; Alam, M. EMHD radiating fluid flow along a vertical Riga plate with suction in a rotating system. *SN Appl. Sci.* **2021**, *3*, 452. [CrossRef]
25. Mallikarjuna, H.B.; Nirmala, T.; Punith Gowda, R.J.; Manghat, R.; Varun Kumar, R.S. Two-dimensional Darcy–Forchheimer flow of a dusty hybrid nanofluid over a stretching sheet with viscous dissipation. *Heat Transf.* **2021**, *50*, 3934–3947. [CrossRef]
26. Koriko, O.K.; Adegbie, K.S.; Shah, N.A.; Animasaun, I.L.; Olotu, M.A. Numerical solutions of the partial differential equations for investigating the significance of partial slip due to lateral velocity and viscous dissipation: The case of blood-gold Carreau nanofluid and dusty fluid. *Numer. Methods Partial. Differ. Equ.* **2021**, ahead of print. [CrossRef]
27. Gireesha, B.J.; Sowmya, G.; Khan, M.I.; Öztop, H.F. Flow of hybrid nanofluid across a permeable longitudinal moving fin along with thermal radiation and natural convection. *Comput. Methods Programs Biomed.* **2020**, *185*, 105166. [CrossRef]
28. Awais, M.; Awan, S.E.; Raja, M.A.; Shoaib, M. Effects of Gyro-Tactic Organisms in Bio-convective Nano-material with Heat Immersion, Stratification, and Viscous Dissipation. *Arab. J. Sci. Eng.* **2020**, *46*, 5907–5920. [CrossRef]
29. Gopal, D.; Saleem, S.; Jagadha, S.; Ahmad, F.; Almatroud, A.O.; Kishan, N. Numerical analysis of higher order chemical reaction on electrically MHD nanofluid under influence of viscous dissipation. *Alex. Eng. J.* **2021**, *60*, 1861–1871. [CrossRef]
30. Aziz, A.; Jamshed, W.; Aziz, T.; Bahaidarah, H.; Ur Rehman, K. Entropy analysis of Powell–Eyring hybrid nanofluid including effect of linear thermal radiation and viscous dissipation. *J. Therm. Anal. Calorim.* **2021**, *143*, 1331–1343. [CrossRef]
31. Jawad, M.; Khan, Z.; Bonyah, E.; Jan, R. Analysis of Hybrid Nanofluid Stagnation Point Flow over a Stretching Surface with Melting Heat Transfer. *Math. Probl. Eng.* **2022**, *2022*, 9469164. [CrossRef]
32. Irfan, M.; Farooq, M.A.; Iqra, T. A New Computational Technique Design for EMHD Nanofluid Flow Over a Variable Thickness Surface with Variable Liquid Characteristics. *Front. Phys.* **2020**, *8*, 66. [CrossRef]
33. Reddisekhar Reddy, S.R.; Bala Anki Reddy, P.; Sandeep, N. Numerical study on slip effects on aligned magnetic field flow over a permeable stretching surface with thermal radiation and viscous dissipation. *IOP Conf. Ser. Mater. Sci. Eng.* **2017**, *263*, 062003. [CrossRef]
34. Tlili, I.; Nabwey, H.A.; Ashwinkumar, G.P.; Sandeep, N. 3-D magnetohydrodynamic AA7072-AA7075/methanol hybrid nanofluid flow above an uneven thickness surface with slip effect. *Sci. Rep.* **2020**, *10*, 4265. [CrossRef] [PubMed]
35. Roberts, L. On the melting of a semi-infinite body of ice placed in a hot stream of air. *J. Fluid Mech.* **1958**, *4*, 505–528. [CrossRef]
36. Wu, L. A slip model for rarefied gas flows at arbitrary Knudsen number. *Appl. Phys. Lett.* **2008**, *93*, 253103. [CrossRef]
37. Divya, A.; Reddy, P.B.A. Electromagnetohydrodynamic unsteady flow with entropy generation and hall current of hybrid nanofluid over a rotating disk: An application in hyperthermia therapeutic aspects. *Proc. Inst. Mech. Eng. Part C J. Mech. Eng. Sci.* **2022**, *236*, 7511–7528. [CrossRef]
38. Bala Anki Reddy, P.; Jakeer, S.; Thameem Basha, H.; Reddy Reddisekhar Reddy, S. Multi-layer artificial neural network modeling of entropy generation on MHD stagnation point flow of Cross-nanofluid. *Waves Random Complex Media* **2022**. ahead of print. [CrossRef]
39. Reddy, P.B.; Salah, T.; Jakeer, S.; Mansour, M.A.; Rashad, A.M. Entropy generation due to magneto-natural convection in a square enclosure with heated corners saturated porous medium using Cu/water nanofluid. *Chin. J. Phys.* **2022**, *77*, 1863–1884. [CrossRef]
40. Kayalvizhi, J.; Vijaya Kumar, A.G. Ramping Wall Boundary Analysis of Buoyant-Driven Convection Magnetohydrodynamics (MHD) Flow of B–H2O and Al2O3–H2O Nanofluid Past Vertical Edge in a Porous Zone. *J. Nanofluids* **2022**, *11*, 879–894. [CrossRef]